Journal of Pathology
J Pathol 2018; **244:** 346–357
Published online 29 January 2018 in Wiley Online Library (wileyonlinelibrary.com) DOI: 10.1002/path.5021

ORIGINAL PAPER

Nrf2 promotes oesophageal cancer cell proliferation via metabolic reprogramming and detoxification of reactive oxygen species

Yuki Kitano[1], Yoshifumi Baba[1], Shigeki Nakagawa[1], Keisuke Miyake[1,2], Masaaki Iwatsuki[1], Takatsugu Ishimoto[1,2], Yo-ichi Yamashita[1], Naoya Yoshida[1], Masayuki Watanabe[3], Mitsuyoshi Nakao[4] and Hideo Baba[1]*

[1] *Department of Gastroenterological Surgery, Graduate School of Medical Sciences, Kumamoto University, Kumamoto, Japan*
[2] *International Research Center for Medical Sciences, Kumamoto University, Kumamoto, Japan*
[3] *Department of Gastroenterological Surgery, Cancer Institute Hospital, Japanese Foundation for Cancer Research, Tokyo, Japan*
[4] *Department of Medical Cell Biology, Institute of Molecular Embryology and Genetics, Kumamoto University, Kumamoto, Japan*

**Correspondence to: Hideo Baba, Department of Gastroenterological Surgery, Graduate School of Medicine, Kumamoto University, 1-1-1 Honjo, Chuo-ku, Kumamoto 860-8556, Japan. E-mail: hdobaba@kumamoto-u.ac.jp*

Abstract

Cancer cells consume a large amount of energy and maintain high levels of anabolism to promote cell proliferation via metabolic reprogramming. Nuclear factor erythroid 2-related factor 2 (Nrf2; NFE2L2) is a master transcription regulator of stress responses and promotes metabolic reprogramming to support cell proliferation in various types of cancer. As oesophageal cancer is one of the most aggressive gastrointestinal cancers, we aimed to clarify the effect of Nrf2 on metabolic reprogramming in oesophageal cancer. The relationship between Nrf2 expression and clinical outcome was evaluated using a database comprising 201 oesophageal cancers. Using *in vitro* assays and metabolome analysis, we examined the mechanism by which Nrf2 affects malignant phenotype. High-level immunohistochemical expression of Nrf2 was significantly associated with poor recurrence-free survival (HR = 2.67, $p = 0.0004$) and overall survival (HR = 2.90, $p < 0.0001$) in oesophageal cancer patients. In an *in vitro* assay with siRNA in TE-11 cells, which showed high Nrf2 expression, Nrf2 depletion significantly decreased cell growth and enhanced G1 cell cycle arrest and apoptosis. In addition, reactive oxygen species (ROS) were not removed by detoxification via the Nrf2 pathway, with concomitant induction of the p38 mitogen-activated protein kinase pathway. The metabolome analysis showed that Nrf2 strongly promoted metabolic reprogramming to glutathione metabolism, which synthesizes the essential fuels for cancer progression. Furthermore, metabolome analysis using oesophageal cancer specimens confirmed that samples displaying high Nrf2 expression promoted glutathione synthesis. Metabolic reprogramming to glutathione metabolism, and ROS detoxification by activation of Nrf2, enhanced cancer progression and led to a poor clinical outcome in oesophageal cancer patients.

Keywords: Nrf2; NFE2L2; glutathione metabolism; ROS detoxification; oesophageal cancer

Received 12 May 2017; Revised 15 November 2017; Accepted 9 December 2017

No conflicts of interest were declared.

Introduction

Oesophageal cancer is the sixth most common cause of cancer-related death worldwide, resulting in approximately 400 000 deaths per year [1]. Despite recent advances in multimodality therapies including chemotherapy, radiotherapy, and chemoradiotherapy, the prognosis of patients, even those who have undergone curative resection, remains poor [2–4]. Further studies are therefore needed to clarify the pathogenesis and biology of oesophageal cancer and to explore new diagnostic and therapeutic possibilities.

Metabolic activities in proliferating cells are fundamentally different from those in quiescent cells. Proliferating cells shunt their metabolites into anabolic pathways, which consume large quantities of nutrients [5]. Utilizing such characteristics of proliferating cells, detection of the glucose analogue 2-[^{18}F]fluoro-2-deoxy-D-glucose by positron emission tomography is by far the most commonly used imaging technique in clinical situations including oesophageal cancer [6–8]. Recent studies have revealed that oncogenic pathways directly promote the metabolism of glucose and glutamine [9–11]. Furthermore, considering that such aberrant activated metabolism in proliferating cells promotes the accumulation of reactive oxygen species (ROS), the efficient detoxification of ROS is a requisite for cancer cell proliferation [12–16]. To counteract the detrimental effects of ROS, cancer cells provide two of the most abundant antioxidants – reduced glutathione (GSH) and reduced nicotinamide adenine dinucleotide phosphate – by genetic changes and metabolic adaptations [16,17].

Nuclear factor erythroid 2-related factor 2 (Nrf2; NFE2L2) is a master transcriptional activator of cytoprotective genes. Although Nrf2 is constantly ubiquitinated by Kelch-like ECH-associated protein 1 (Keap1) under normal conditions [18,19], it is constantly stabilized in various human cancers and confers a growth advantage on cancer cells by enhancing cytoprotection and anabolism [10,12,20–22]. Cancers with high Nrf2 levels are associated with poor prognosis through various mechanisms [21,23–25]. Recent reports have revealed that Nrf2 promotes metabolic reprogramming of various metabolic pathways to maintain the aggressiveness of cancer progression [10,26–28], and the Nrf2 pathway characterizes one molecular subtype of oesophageal squamous cell carcinoma [29]. However, no study has examined the prognostic impact of Nrf2 from the view of cancer metabolism in oesophageal cancer. Based on previous evidence, we hypothesized that Nrf2 is one of the metabolic regulators in oesophageal cancer and affects the aggressive malignant phenotype.

To test this hypothesis, we examined the prognostic impact of Nrf2 expression using a cohort of 201 oesophageal cancers, and performed functional and metabolome analysis utilizing oesophageal cancer cell lines with a small interfering RNA (siRNA) technique and resected specimens.

Materials and methods

Study group

We recruited 361 oesophageal cancer patients who underwent curative resection with radical lymph node dissection at Kumamoto University Hospital between April 2005 and December 2012. Among the 361 candidates, 160 were excluded because they had undergone preoperative treatment. We obtained paraffin-embedded sections from the 201 eligible oesophageal cancer patients' tissue samples. The patients were followed up at 1- to 3-month intervals until death or 31 January 2016, whichever came first. Tumour staging was based on the criteria of the American Joint Committee, specified in the *Cancer Staging Manual*, 7th edition [30]. Overall survival (OS) was defined as the time between the operation date and the date of death. Recurrence-free survival (RFS) was defined as the time between the operation date and the date of recurrence or death. Written informed consent was obtained from each subject, and the study procedures were approved by the Institutional Review Board of Kumamoto University.

Reverse transcription–quantitative PCR (RT-qPCR)

Total RNA extraction, cDNA synthesis, and RT-qPCR were carried out as previously described [31]. The RT-qPCR primers were designed using the Universal Probe Library (Genenet, Fukuoka, Japan) following the manufacturer's recommendations. The primer sequences and probes used are shown in the supplementary material, Table S1.

Immunohistochemistry and evaluation

Paraffin-embedded tumour sections were dewaxed in xylene and ethanol, and autoclaved for 15 min in antigen retrieval solution (pH 7.0, RM102-H; LSI Medience, Tokyo, Japan) to retrieve their antigen epitopes and then allowed to cool. Primary antibodies against Nrf2 (1:200 dilution; sc-365949; Santa Cruz Biotechnology, Dallas, TX, USA), cyclin D1 (1:50 dilution; PA00046; Leica Biosystems, Newcastle, UK), and Ki-67 (1:75 dilution; M7240; Dako, Tokyo, Japan) were applied. The secondary antibody was a ready-for-use anti-mouse EnVision-Peroxidase system (EnVision1 kit; Dako) applied for 30 min at 25 °C and incubated in 3,3'-diaminobenzidine tetrahydrochloride at 25 °C for 10 min. The stained slides were counterstained with haematoxylin and bluing reagent. Nrf2, cyclin D1, and Ki-67 staining was analysed by two authors (YK and YB) who were unaware of the clinical data. Immunohistochemical soring of Nrf2 and cyclin D1 was conducted by multiplying the staining intensity by the staining extent. The staining intensity was assigned a score of 0, 1, 2, or 3, denoting negative, weak, moderate, or strong staining, respectively. The staining extent was defined as the rate of positively stained cancer cells (0–1.0). Based on the median Nrf2 score (1.0), the patients were divided into two groups, a low-Nrf2 group (0–0.99, $n = 110$) and a high-Nrf2 group (1.0–2.1, $n = 91$), for further analysis (supplementary material, Figure S1A). Ki-67 staining was scored by counting the proportion of positively stained cells.

Cell lines

Human oesophageal cancer cell lines were obtained from the Cell Resource Center for Biomedical Research, Institute of Development, Aging and Cancer, Tohoku University, Japan; the Riken BioResource Center Cell Bank, Ibaraki, Japan; and the Japanese Collection of Research Bioresources Cell Bank, Osaka, Japan. They were cultured in 5% CO_2 at 37 °C in RPMI 1640 medium supplemented with 10% fetal bovine serum. The cell lines had been tested and authenticated by the Cell ID System in October 2013.

Depletion of Nrf2 by synthetic small interfering RNAs (siRNAs)

Two individual Nrf2-specific siRNAs were chemically synthesized (Invitrogen, Tokyo, Japan). Stealth RNAi negative control (Invitrogen) was used as a negative control. The concentration of the siRNA was set at 5 nM to cause less than 20% inhibition of Nrf2. Twenty-four hours after plating, the cells were transfected using 5 nM Nrf2-siRNAs or control siRNA using the Lipofectamine transfection reagent RNAiMAX (Invitrogen) in accordance with the manufacturer's instructions.

Western blotting

Protein extraction from cultivated cells and western blot analyses were carried out as previously described

[31]. Primary antibodies for Nrf2 (1:1000 dilution; ab62352; Abcam, Cambridge, UK), Keap1 (1:1000 dilution; ab218815; Abcam), caspase-3 (1:1000 dilution; #9662; Cell Signaling, Danvers, MA, USA), p38 mitogen-activated protein kinase (MAPK) (1:1000 dilution; #8690; Cell Signaling), phospho-p38 MAPK (1:1000 dilution; #9215; Cell Signaling), cyclin D1 (1:1000 dilution; PA00046; Leica Biosystems), and β-actin (1:1000 dilution; #4967; Cell Signaling) were used in this study. We performed western blotting in triplicate, and quantification using ImageJ, with statistical evaluation, is shown.

Growth assay

Cells were seeded in a 96-well plate at a density of 3000 cells per well at 24 h after transfection with the two siRNAs. Viable oesophageal cancer cell numbers were measured with a Cell Counting Kit-8 (Dojin Laboratories, Kumamoto, Japan) at 24, 48, 72, and 96 h. Optical density (OD) at 450 nm was measured using an automatic microplate reader (Molecular Devices, Osaka, Japan). Each experiment was performed in triplicate.

Flow cytometric analysis of cell cycle distribution and detection of apoptosis

Twenty-four hours after transfection with the two siRNAs, the cells were trypsinized, adjusted to 1.0×10^6 cells/ml, and fixed with 70% ethanol. They were then pelleted and resuspended in phosphate-buffered saline containing 1 μg/ml RNase A (Sigma, Tokyo, Japan) and 100 μg/ml propidium iodide (PI) (Sigma). Cell cycle analyses were performed using a FACS Verse flow cytometer (BD Biosciences, Tokyo, Japan). The distribution of cells in different cell cycle phases was calculated using FlowJo software (TOMY Digital Biology, Tokyo, Japan). Phosphatidylserine externalization was detected by annexin V staining (Millipore, Tokyo, Japan) following the manufacturer's instructions. Annexin V-positive and PI-negative cells were scored as early apoptotic cells.

Reactive oxygen species (ROS) detection and measurement

Intracellular ROS levels were measured by staining with CellROX Green Reagent (Thermo Fisher Scientific, Waltham, MA, USA) and CM-H2DCFDA (Thermo Fisher Scientific). Cells were seeded in a six-well plate at a density of 2.0×10^5 cells per well at 24 h after transfection. CellROX Green Reagent was added to the medium to a concentration of 5 μM for 30 min at 37 °C, after which the medium was removed and cells were washed three times with PBS. Images were captured using a Biorevo BZ-X700 fluorescence microscope (Keyence, Tokyo, Japan) and analysis software.

Bioinformatic analysis

The mutation status of oesophageal cancer cell lines was obtained from the Catalogue of Somatic Mutations in Cancer (COSMIC) database and Cancer Cell Line Encyclopedia (CCLE) project. The public datasets GSE23400, GSE33103, GSE47404, and GSE66258, and the Cancer Genome Atlas (TCGA) dataset were used for bioinformatic analysis. GSEA (Gene Set Enrichment Analysis: http://software.broadinstitute.org/gsea/index.jsp) was used for the assessment of a gene set's enrichment. In GSEA, the upper 25th percentile was considered as the Nrf2-high expression group and compared with the Nrf2-low expression group. Gene sets in the Kyoto Encyclopedia of Genes and Genomes (KEGG) and HALLMARK were used for enrichment analysis.

Metabolite measurements and metabolomic profiling of cultured cells

To measure the levels of intracellular metabolites, TE-11 cells were prepared at $1–3 \times 10^7$ cells per sample at 48 h after siRNA transfection. Datasets were acquired on a liquid chromatography (LC) system (Agilent 1260 Series; Agilent Technologies, Palo Alto, CA, USA) equipped with a CAPCELL PAK C18 IF column [2.0 mm ID (inner diameter) × 50 mm, 2 μm; Shiseido, Tokyo, Japan] and a capillary electrophoresis (CE) system (Agilent CE; Agilent Technologies) equipped with a polymicro tube column (50 μm ID × 1000 mm; GL Science, Tokyo, Japan), coupled to an electrospray ionization quadrupole time-of-flight (Q-TOF) mass spectrometer (MS) (Agilent 6520, Agilent Technologies). Cells were snap-frozen in liquid nitrogen and homogenized using a Multi-beads Shocker homogenizer. The homogenates were mixed with 2 ml of methanol and 2 ml of chloroform and shaken. The aqueous layer was collected by centrifugation at 1000 × *g* for 15 min and dried at 30 °C using a Turbo Vap (Turbo Vap LV, Biotage, Japan). Dried extracts were mixed with 200 μl of 10% acetonitrile solution. For analysis by LC–MS, 120 μl of lysate was mixed with 30 μl of internal standard (IS). For analysis of CE–MS, 60 μl of lysate was mixed with 15 μl of IS and filtered by centrifugation at 10 000 × *g* for 10 min. After the analysis, the values were normalized by sample amount. Each experiment was performed in triplicate.

Statistical analyses

Continuous variables were expressed as mean ± standard deviation; differences were assessed for significance using Student's *t*-test or the Mann–Whitney test. Categorical variables were evaluated using chi-square or Fisher's exact tests, as appropriate. Cox proportional hazards regression analyses were performed to identify predictors of prognosis. RFS and OS rates were estimated using the Kaplan–Meier method, and survival curves were compared using the log-rank test. $p < 0.05$ was considered significant. All tests were performed using JMP software version 10.0.2 (SAS Institute, Cary, NC, USA).

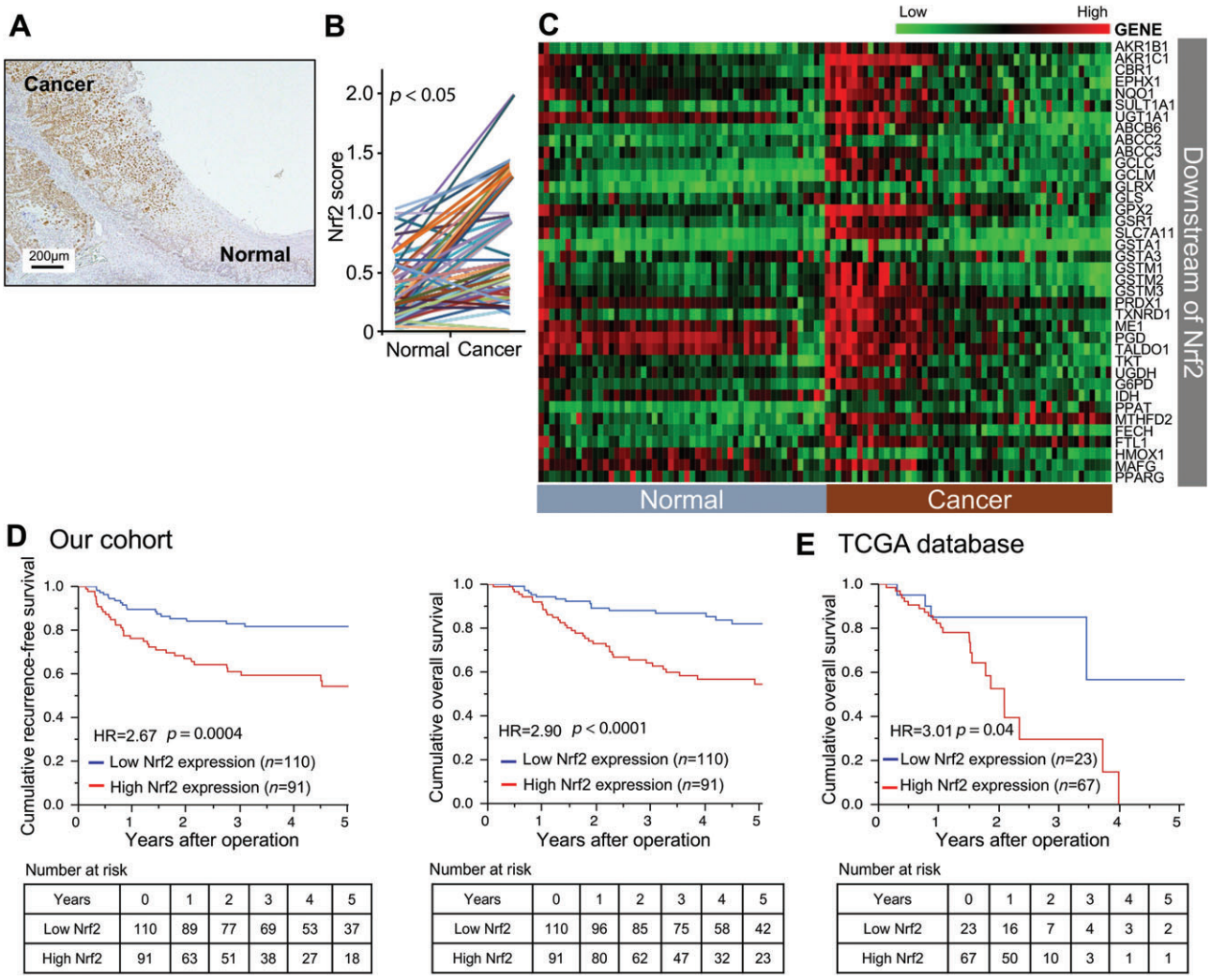

Number at risk

Years	0	1	2	3	4	5
Low Nrf2	110	89	77	69	53	37
High Nrf2	91	63	51	38	27	18

Number at risk

Years	0	1	2	3	4	5
Low Nrf2	110	96	85	75	58	42
High Nrf2	91	80	62	47	32	23

Number at risk

Years	0	1	2	3	4	5
Low Nrf2	23	16	7	4	3	2
High Nrf2	67	50	10	3	1	1

Figure 1. Expression of Nrf2 in oesophageal cancer tissues and matched non-cancerous oesophageal mucosae, and patients' prognosis by Nrf2 in cancer tissue. (A) Immunohistochemistry for Nrf2 expression in oesophageal cancer tissues and matched non-cancerous oesophageal mucosae. (B) Comparison of Nrf2 expression levels in cancer tissues and matched non-cancerous oesophageal mucosae sampled from 201 oesophageal cancer patients. (C) Heatmap of downstream genes controlled by Nrf2 in oesophageal cancer tissues and matched non-cancerous oesophageal mucosae, calculated from GEO profiles (GSE23400, $n = 53$). (D) Kaplan–Meier curves of recurrence-free survival and overall survival in oesophageal cancer patients with high and low expression of Nrf2, calculated from our cohort ($n = 201$). (E) Kaplan–Meier curves of overall survival in oesophageal squamous cell carcinoma patients with high and low expression of Nrf2, calculated from the TCGA database ($n = 90$).

Results

Clinical and prognostic features of Nrf2 expression in oesophageal cancer patients

Using immunohistochemistry, we examined the protein level of Nrf2 in cancer tissues and the matched non-cancerous mucosae of 201 oesophageal cancer patients. Nrf2 immunoreactivity in cancer tissue was significantly stronger than in matched non-cancerous mucosa ($p < 0.05$; Figure 1A, B). In addition, utilizing Gene Expression Omnibus (GEO) profiles (GSE23400), we confirmed that the expression of important genes controlled by Nrf2 was higher in cancer tissue than in non-cancerous mucosa (Figure 1C). These genes were collected from a previous review [32]. Supplementary material, Table S2 shows the relationship between Nrf2 expression status and clinicopathological features. High-level Nrf2 expression was significantly associated with male sex ($p = 0.02$), a higher value of standardized uptake value max ($p = 0.048$), and advanced T stage ($p = 0.01$), N stage ($p = 0.002$), and tumour stage ($p = 0.001$) (supplementary material, Table S2). There were 59 deaths among the 201 oesophageal cancer patients. The median follow-up time for censored patients was 3.7 years. In Kaplan–Meier analysis, high Nrf2 expression was significantly associated with worse clinical outcomes (RFS: HR = 2.67, $p = 0.0004$; OS: HR = 2.90, $p < 0.0001$; Figure 1D). To evaluate the robustness of our findings, we analysed survival status using the TCGA database as a validation cohort and observed similar results: high Nrf2 expression patients experienced a significantly worse prognosis (HR = 3.01, $p = 0.04$; Figure 1E). Multivariate analysis showed that performance status (PS) 1 or 2 (HR = 3.54, $p < 0.0001$), microlymphatic

Table 1. Cox regression analysis for overall survival in patients with oesophageal cancer who underwent surgery

	Univariate analysis			Multivariate analysis		
Variable	HR	95% CI	*P* value	HR	95% CI	*P* value
Age ≥ 65 years	1.41	0.84–2.39	0.19			
Male	1.07	0.50–2.79	0.88			
PS 1–2	3.17	1.81–5.39	**< 0.0001**	3.54	1.94–6.33	**< 0.0001**
BMI ≥ 22	0.76	0.45–1.28	0.30			
Brinkman index ≥750	0.81	0.48–1.36	0.43			
Alcohol use present	0.63	0.33–1.28	0.19			
Comorbidity present	1.22	0.71–2.19	0.47			
Double cancer present	1.36	0.79–2.29	0.26			
Upper tumour location	0.72	0.43–1.20	0.20			
Tumour size ≥40 mm	1.93	1.13–3.35	**0.02**	1.13	0.60–2.14	0.70
Tumour stage III–IV	2.56	1.52–4.34	**0.0006**	1.55	0.77–3.11	0.22
Microlymphatic invasion positive	2.36	1.39–3.94	**0.002**	2.08	1.07–4.01	**0.03**
Microvascular invasion positive	2.07	1.23–3.52	**0.006**	1.37	0.76–2.53	0.30
Adjuvant therapy	1.10	0.63–1.87	0.73			
Nrf2-high expression	2.90	1.71–5.09	**< 0.0001**	2.57	1.44–4.74	**0.001**

PS = performance status; BMI = body mass index; HR = hazard ratio; CI = confidence interval.
Bold values are statistically significant at $p < 0.05$.

invasion-positive (HR = 2.08, $p = 0.03$), and high Nrf2 expression (HR = 2.57, $p = 0.001$) were independent prognostic factors for OS (Table 1). We examined whether the influence of Nrf2 on OS was modified by any of the clinical, pathological, or epidemiological variables evaluated. However, the effect of Nrf2 was not significantly modified by any clinicopathological features (all $p > 0.05$; supplementary material, Figure S1B).

Nrf2 expression levels in oesophageal cancer cell lines and Nrf2 depletion by siRNA

To evaluate how Nrf2 affects cancer progression and patients' clinical outcome, we performed an *in vitro* assay using oesophageal cancer cell lines. We determined the mRNA levels of *Nrf2*, and protein expression of Nrf2 and Keap1, in ten oesophageal cancer cell lines by RT-qPCR and western blotting (Figure 2A, B). Moreover, we examined the mutation status of these cell lines from the COSMIC database and CCLE project (supplementary material, Figure S2A). Among these cell lines, we selected TE-1 cells for low Nrf2 protein level, TE-9 cells for high level with wild type of both Nrf2 and Keap1, and TE-11 cells for high level with both mutations. We confirmed that siRNAs for Nrf2 (siNrf2 #1 and siNrf2 #3) effectively suppressed Nrf2 expression at 24 and 48 h after transfection of siRNA, at both mRNA and protein levels (supplementary material, Figure S2B, C).

Nrf2 depletion results in growth inhibition due to G1 cell cycle arrest and induction of apoptosis

To assess whether Nrf2 regulates oesophageal cancer cell proliferation, we performed a cell growth assay using oesophageal cancer cell lines, comparing control and Nrf2 depletion cells. The numbers of cells were significantly decreased by Nrf2 depletion in all cell lines, particularly in TE-11 cells (Figure 2C, D). Flow cytometric cell cycle analysis using PI staining showed significant increases in G0/G1 populations and concomitant decreases in S-phase populations as a result of Nrf2 depletion in both TE-9 and TE-11 cells, but TE-1 cells did not display significant differences (Figure 3A). Representative flow cytometric curves are shown in the supplementary material, Figure S3. Taken together, these results indicate that Nrf2 depletion induces cell cycle arrest in the G0/G1 phase and inhibits the growth of oesophageal cancer cells that express Nrf2 relatively highly. Next, we examined the effects of Nrf2 depletion on apoptosis in oesophageal cancer cells. Flow cytometric analysis revealed that although Nrf2-depleted TE-11 cells showed an increase in active caspase-3 staining compared with control cells, TE-1 and TE-9 cells showed no difference (Figure 3B). Furthermore, western blotting analysis also showed that Nrf2-depleted TE-11 cells displayed an increase in the protein expression of cleaved caspase-3, and the difference was significant (Figure 3C and supplementary material, Figure S4). By flow cytometric analysis using annexin V and PI staining, we found that the number of early apoptotic cells was increased by Nrf2 depletion only in TE-11, and not in TE-1 or TE-9 cells, compared with control cells (Figure 3D). In addition, the sub-G1 phase population indicating apoptotic cells was also increased by Nrf2 depletion in TE-11 cells only (Figure 3E). Together, these results indicate that Nrf2 depletion induces apoptosis in cells expressing Nrf2 at a high level.

Nrf2 controls ROS detoxification and inhibits the p38 MAPK pathway

To assess Nrf2-mediated ROS detoxification, we examined the effect of Nrf2 depletion on the production of ROS. We used the CellROX Green Reagent, which can detect ROS in nuclei and mitochondria [33] because ROS generated by mitochondria move to the nucleus and participate in various signalling pathways in cancer cells [17]. In our analysis, ROS were detected in the nucleus in TE-11 (supplementary material, Figure

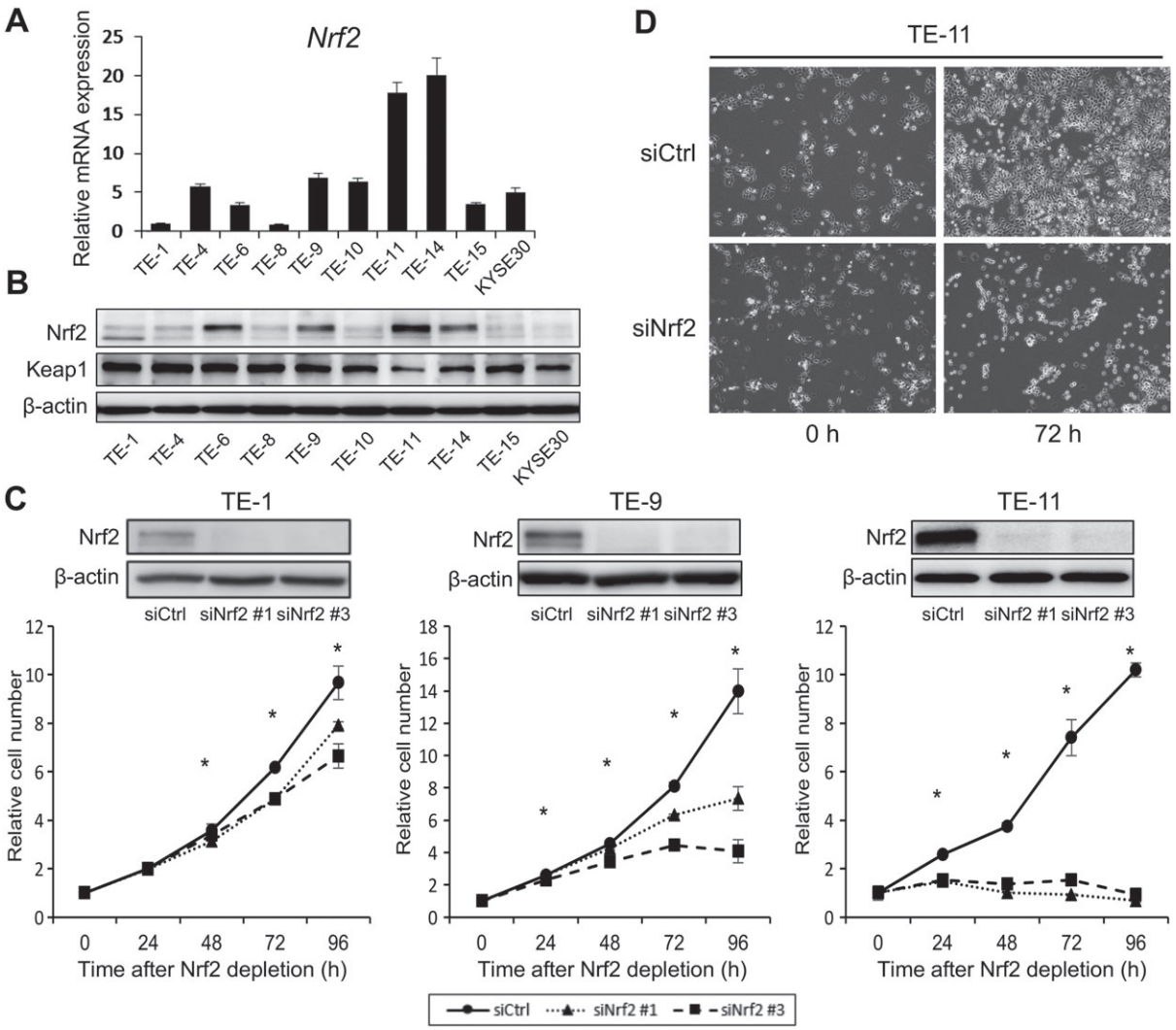

Figure 2. Expression of Nrf2 in oesophageal cancer cell lines, and cell growth assay in TE-1, -9, and -11 cells, treated with siCtrl and siNrf2. (A) mRNA levels of *Nrf2* in oesophageal cancer cell lines, determined by RT-qPCR. (B) Protein levels of Nrf2 and Keap1 in the same cell lines, determined by western blotting analysis. (C) Cell growth assay in TE-1, -9, and -11 cells following the indicated treatment. (D) Comparison of cell growth in TE-11 following the indicated treatment, visualized by time-lapse imaging. Experiments were performed in triplicate. Standard deviations are indicated. $^*p < 0.05$.

S5A). Although control cells could remove ROS, Nrf2-depleted cells could not, and the difference was significant in TE-11 (Figure 4A, B). However, in TE-1, the level of ROS did not differ between control and Nrf2-depleted cells (Figure 4B and supplementary material, Figure S5B). Furthermore, from another method of ROS assessment using CM-H2DCFDA, a similar result was observed in both cells (Figure 4C). To evaluate the antioxidant responses, we assessed the glutathione redox couple GSH/GSSG (GSSG: oxidized glutathione), which can indicate the appropriate cellular redox status and is decreased under oxidative stress conditions because glutathione peroxidase reduces H_2O_2 to water while it oxidizes GSH to GSSG [17,34]. GSH/GSSG was decreased significantly by Nrf2 depletion in TE-11 cells compared with control cells (Figure 4D). To clarify which pathway affected cell proliferation in response to accumulation of ROS, we focused on the MAPK pathway. p38 MAPK is a stress-activated protein kinase that is activated by environmental and genotoxic stress [35–37]. We showed by western blotting that Nrf2 depletion induced p38 MAPK phosphorylation and inhibited the expression of cyclin D1 in TE-11, but this change did not occur in TE-1 (Figure 4E); the statistical evaluations are shown in the supplementary material, Figure S4. Moreover, to reveal the importance of phosphorylated p38 MAPK for the Nrf2 pathway, we showed that inhibiting the phosphorylation of p38 MAPK by administration of the p38 MAPK inhibitor SB203580 (Selleckchem, Houston, TX, USA) increased the expression of cyclin D1 in Nrf2-depleted cells and did not change the expression of Nrf2 (Figure 4F). Furthermore, Nrf2-depleted cells could recover their growth ability by inhibition of the phosphorylation of p38 MAPK (Figure 4G). These results revealed that the phosphorylation of p38 MAPK was important for cancer progression caused by the Nrf2 pathway and that the phosphorylation of p38 MAPK

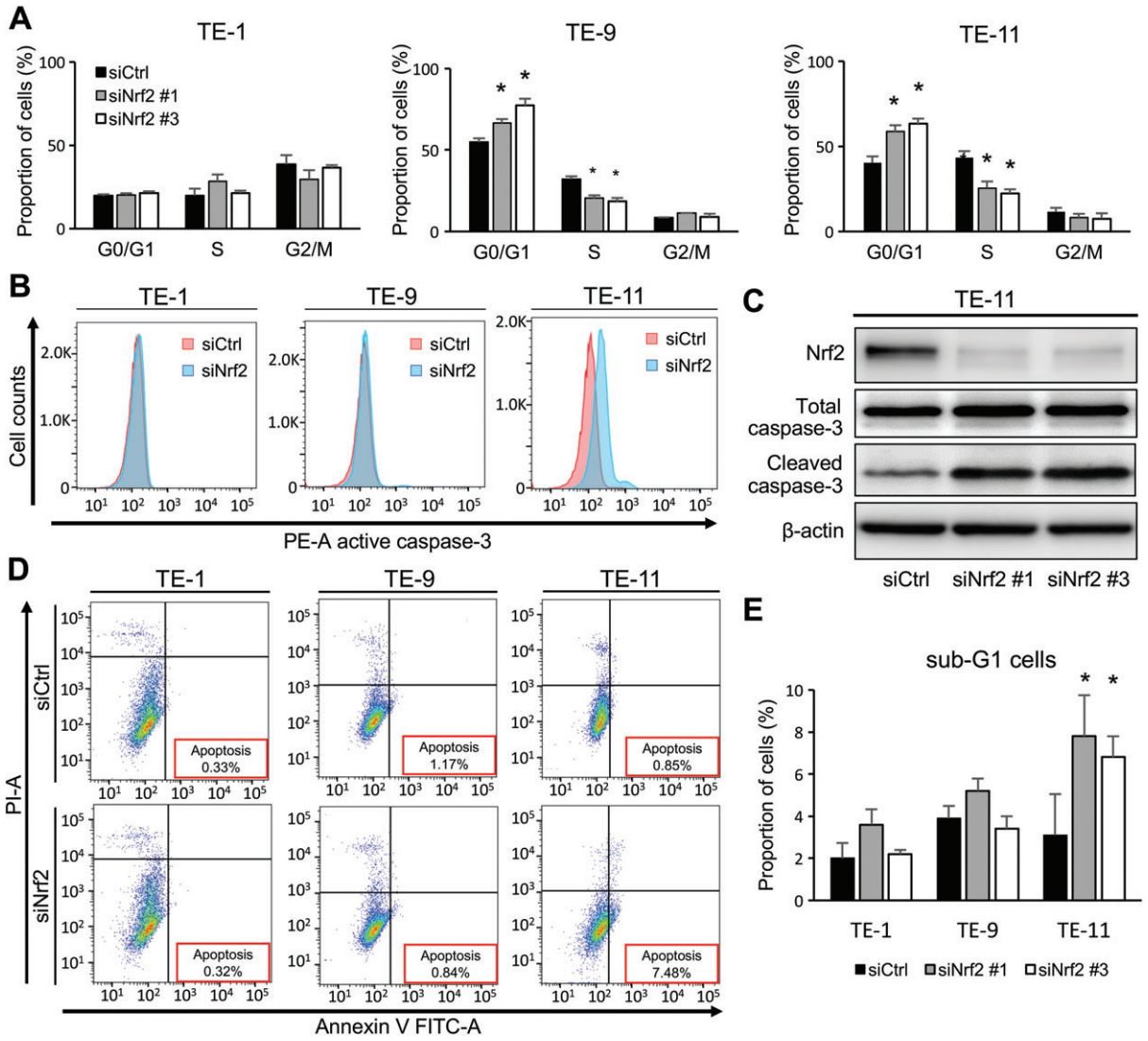

Figure 3. Comparison of cell cycle and apoptosis in TE-1, -9, and -11 cells treated with siCtrl and siNrf2. (A) Cell cycle assay in TE-1, -9, and -11 cells following the indicated treatment, performed by flow cytometry. (B) Level of active caspase-3 in TE-1, -9, and -11 cells following the indicated treatment, assessed by flow cytometry. (C) Protein expression of caspase-3 in TE-11 cells following the indicated treatment, analysed by western blotting. (D) Apoptosis assay in TE-1, -9, and -11 cells following the indicated treatment, assessed by staining with PI and annexin V. (E) Apoptosis evaluated by quantifying the sub-G1 population from a cell cycle assay in TE-1, -9, and -11 cells following the indicated treatment. Experiments were performed in triplicate. Standard deviations are indicated. *$p < 0.05$.

itself did not affect Nrf2 activation. Furthermore, we evaluated immunohistochemically the expression of cyclin D1 and Ki-67 in oesophageal cancer tissues and found that the high-Nrf2 group had significantly higher cyclin D1 and Ki-67 expression than the low-Nrf2 group ($p < 0.05$) (Figure 4H and supplementary material, Figure S5C). These results indicate that Nrf2 depletion suppresses cell proliferation via accumulation of ROS and activation of the p38 MAPK pathway in cells expressing high levels of Nrf2.

Nrf2 induces metabolic reprogramming to glutathione metabolism

To elucidate the contribution of Nrf2 to metabolic reprogramming, we performed a metabolome analysis in TE-11 cells treated with siCtrl and siRNA, using an LC–MS and CE–MS system. Interestingly, Nrf2 depletion significantly decreased the level of GSH (Figure 5A, B) and changed the levels of intermediates and amino acids related to glutathione synthesis (Figure 5B and supplementary material, Figure S6A). The glutathione metabolic pathway is shown in Figure 5C. In TE-11 cells with Nrf2 depletion, the level of cysteine decreased because the cysteine transporter xCT (SLC7A11; solute carrier family 7 member 11) is regulated by Nrf2 [10,32]. Meanwhile, glutamate accumulated because glutamate-cysteine ligase modifier subunit (GCLM) and glutamate-cysteine ligase catalytic subunit (GCLC), which catalyse the synthesis of GSH, were regulated by Nrf2 (Figure 5C, D) [10,32]. As a result, the levels of γ-glutamylcysteine, an intermediate in GSH synthesis, and GSH were decreased (Figure 5B). However, the levels of glycine

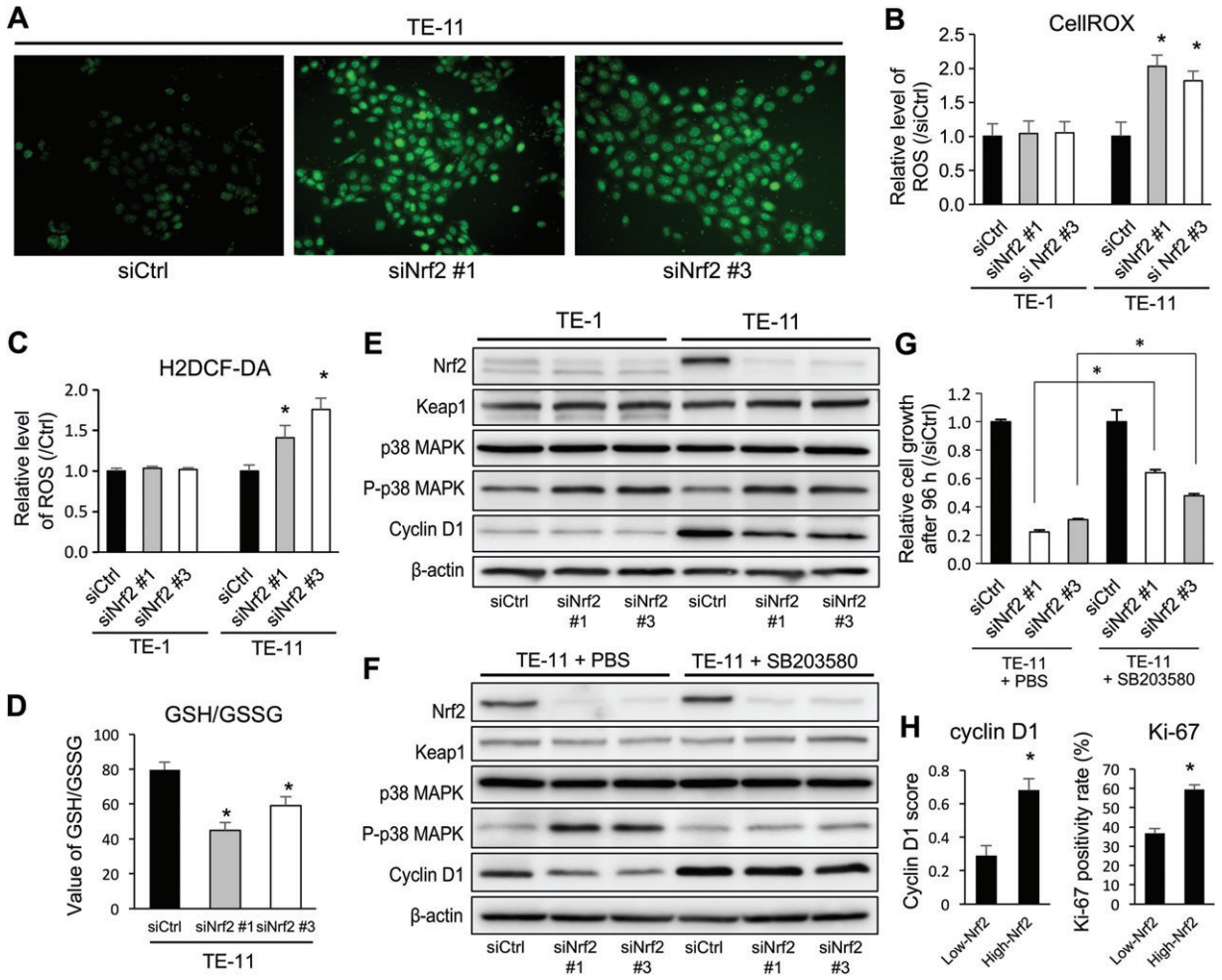

Figure 4. Inhibition of ROS detoxification and activated p38 MAPK pathway in TE-1 and TE-11 cells treated with siNrf2. (A) ROS detection assay using CellROX Green Reagent in TE-11 cells treated with siCtrl and siNrf2. (B) Quantification of ROS detection assay in TE-1 and TE-11 using CellROX Green Reagent following the indicated treatment. (C) Quantification of ROS detection assay in TE-1 and TE-11 using H2DCF-DA following the indicated treatment, performed by flow cytometry. (D) Comparison of GSH/GSSG ratios in TE-11 following the indicated treatment. (E) Expression of p38 MAPK and cyclin D1 in TE-1 and TE-11 following the indicated treatment, by western blotting analysis. (F) Expression of p38 MAPK and cyclin D1 in TE-11 following the indicated treatment and administration of the p38 MAPK inhibitor SB203580, by western blotting analysis. (G) Relative cell growth rate of TE-11 following the indicated treatment with administration of the p38 MAPK inhibitor SB203580. (H) Comparison of immunohistochemistry of cyclin D1 and Ki-67 expression in resected oesophageal cancer tissues between low and high Nrf2 expression. Experiments were performed in triplicate. Standard deviations are indicated. *$p < 0.05$.

were not changed by depletion of Nrf2 because Nrf2 does not regulate glutathione synthase (GSS). Furthermore, GSEA analysis of KEGG pathways with GEO profiles (GSE23400, GSE33103, GSE47404, and GSE66258) showed that the glutathione metabolism gene set was significantly enriched in high-Nrf2 expression cases (Figure 5E, F and supplementary material, Table S3). Moreover, GSEA analysis of HALLMARKS gene sets using GEO23400 showed that the ROS pathway (NES = 1.58, $p = 0.02$) and apoptosis pathway (NES = −1.55, $p < 0.0001$) were significantly enriched in high-Nrf2 expression cases (Figure 5F). We measured the levels of GSH synthesis in 20 resected oesophageal cancer tissues and three cell lines (TE-1, -9, -11) to validate our findings. We found that the levels of GSH in high-Nrf2 cases were significantly higher than in low-Nrf2 cases ($p = 0.009$; Figure 5G), and that the GSH level in each cell line correlated with the protein level of Nrf2 ($p < 0.05$; Figure 2B and supplementary material, Figure S6B).

Discussion

Cancer metabolism has been extensively researched as a potential therapeutic target, and recent studies have suggested that Nrf2 regulates cancer metabolism in several types of cancers [10,26–28]. Thus, a better understanding of the relationship between Nrf2 expression, malignant behaviour, and cancer metabolism in oesophageal cancer may be increasingly important. First, using our own cohort with 201 oesophageal cancers and public databases, we found that high expression of Nrf2 was significantly associated with poor clinical outcome. Second, metabolome analysis using oesophageal cancer cell lines and resected tumour samples showed that high

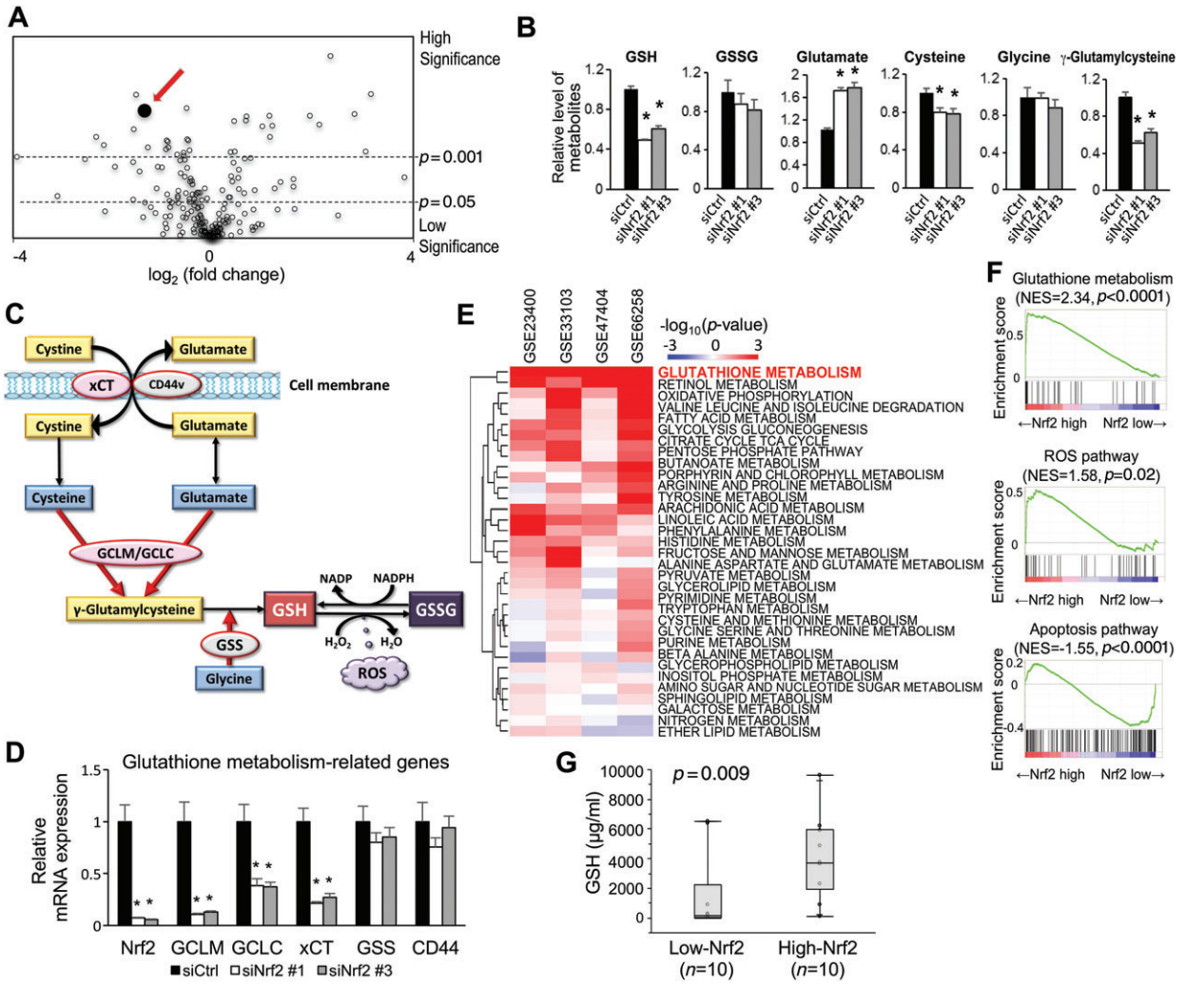

Figure 5. Metabolic reprogramming of glutathione metabolism by Nrf2 in oesophageal cancer cell lines and resected tumours. (A) Volcano plot of metabolites contained in TE-11 cells treated with siNrf2, compared with siCtrl. Arrow shows the level of GSH. (B) Quantification of metabolic intermediates in glutathione metabolism. Metabolite concentrations were quantified at 48 h after siNrf2 transfection. (C) Metabolic pathway and related enzymes of glutathione metabolism. (D) Effects of Nrf2 depletion on gene expression of glutathione metabolism-related enzymes in TE-11 cells. (E) Heatmaps of KEGG metabolic pathways enriched in high Nrf2 expression, calculated by GSEA analysis of KEGG pathways with GEO profiles (GSE23400, GSE33103, GSE47404, and GSE66258). (F) Enrichment score of glutathione metabolism, ROS pathway, and apoptosis pathway from GSEA analysis of KEGG and HALLMARKS gene sets using GEO23400. (G) Quantification of GSH in 20 resected oesophageal cancer tissues between low and high Nrf2 expression. Experiments were performed in triplicate. Standard deviations are indicated. $^*p < 0.05$.

Nrf2 expression correlated with higher levels of GSH. Third, we revealed that Nrf2 promoted cancer cell proliferation and ROS detoxification in an *in vitro* assay. To the best of our knowledge, this study provides the first evidence for the potential of Nrf2 as a regulator of cancer metabolism and for the prognostic impact of Nrf2 in oesophageal cancer.

As mentioned in a review of next-generation hallmarks of cancer, metabolic reprogramming is likely to be involved in the pathogenesis of some and perhaps all cancers [38]. To develop into an aggressive malignant disease, tumour cells must generate energy, which is required to support cell division and to evade the checkpoints that would normally block cell proliferation under the stressful condition [5,38]. In the early 20th century, Otto Warburg suggested that core cellular metabolism was altered during the process of malignant transformation [39]. During the past two decades, it has become clear that various metabolic pathways that are affected by genetic mutations and the tumour microenvironment have a profound effect on cancer metabolism [16,38]. Mitsuishi *et al* revealed that Nrf2 promoted both the pentose phosphate pathway (PPP) and under the sustained activation of PI3K–Akt signalling, and this metabolic shift supported cell proliferation in addition to enhancing cytoprotection [10]. Since that report, although several studies revealed that Nrf2 promoted various metabolic pathways and promoted cell proliferation [26–28], no studies have shown the metabolic significance of Nrf2 in oesophageal cancer. Moreover, although previous studies investigating the significance of Nrf2 in oesophageal cancer showed that genetic mutation and tumour suppressor microRNA targeting Nrf2 correlated with poor prognosis, they

included small numbers of cases and the mechanisms by which Nrf2 induced cancer cell proliferation and poor clinical outcome were not clarified [40–42]. In our study, we examined a large cohort of more than 200 cases and showed, by metabolome analysis, that Nrf2 strongly promoted glutathione metabolism in oesophageal cancer. Collectively, our findings indicate that high Nrf2 expression is significantly associated with cell proliferation and poor clinical outcome in oesophageal cancer.

GSH is the most important hydrophilic antioxidant in our body and protects cells against exogenous and endogenous toxins, including ROS and nitrogen species [34,43]. However, previous studies revealed that GSH is also critical for cell proliferation [44] and drug resistance in cancer cells [45,46]. GSH is a tripeptide that is synthesized *de novo* from the precursor amino acids cysteine, glutamate, and glycine. Furthermore, the three major determinants of GSH synthesis are the availability of cysteine, the activity of the rate-limiting enzyme glutamate cysteine ligase (GCL), and the activity of GSS [47]. Previously, we showed that a CD44 variant interacts with xCT and controls the intracellular level of cysteine and GSH, and this regulation may support ROS defence and tumour growth [44]. In the present study, we showed that Nrf2 could control two determinants of GSH. First, Nrf2 regulated the expression of xCT and controlled the intracellular level of cysteine. Second, Nrf2 regulated the expression of GCLM and GCLC, and finally controlled the synthesis of γ-glutamylcysteine and GSH. We also showed that Nrf2 regulated genes related to glutathione metabolism in *in vitro* and GSEA analysis of KEGG pathways with GEO profiles, and that high-Nrf2 expression cases had higher levels of GSH than low-Nrf2 expression cases, using clinical samples and oesophageal cancer cell lines. In a previous report, Mitsuishi *et al* revealed that in the A549 cell line, Nrf2 promoted both the PPP and the glutathione pathways [10]. However, our study showed that in an oesophageal cancer cell line, Nrf2 promoted not the PPP but rather the glutathione pathway, based on metabolome analysis and *in silico* analysis (Figure 5E and supplementary material, Figure S6C). Furthermore, we showed that the accumulation of ROS by depletion of Nrf2 induced apoptosis and G1 cell cycle arrest via phosphorylation of the p38 MAPK pathway.

In conclusion, Nrf2 reinforces the malignant behaviour of oesophageal cancer cells by up-regulating their proliferative activity, and by inducing glutathione metabolism and ROS detoxification. These mechanisms may be exploited in cancer therapeutics. Future studies are needed to confirm our findings and to examine other potential mechanisms by which Nrf2 affects tumour behaviour.

Acknowledgements

We thank Yoko Ogata and Hiroko Taniguchi for their valuable technical assistance. This work was supported in part by a Grant-in-Aid for Scientific Research from the Japan Society for the Promotion of Science (grant number 26713042).

Author contributions statement

The authors contributed in the following way: conception and design: YK, YB, TI, NY; development of methodology: YK, YB, KM; acquisition of data (provided animals, acquired and managed patients, provided facilities, etc): YB, KN, NY; analysis and interpretation of data (e.g. statistical analysis, biostatistics, computational analysis): YK, YB, SN, KM; writing, review, and/or revision of the manuscript: YK, YB, TI, YY, MW, MN, HB; administrative, technical, or material support (i.e. reporting or organizing data, constructing databases): YK, SN, KM, TI, MI, YS, YY, NY, MW, MN, HB; study supervision: MI, TI, NY, MW, MN, HB.

References

1. Ferlay J, Soerjomataram I, Dikshit R, *et al.* Cancer incidence and mortality worldwide: sources, methods and major patterns in GLOBOCAN 2012. *Int J Cancer* 2015; **136:** E359–E386.
2. Kleinberg L, Forastiere AA. Chemoradiation in the management of esophageal cancer. *J Clin Oncol* 2007; **25:** 4110–4117.
3. Brucher BL, Swisher SG, Konigsrainer A, *et al.* Response to preoperative therapy in upper gastrointestinal cancers. *Ann Surg Oncol* 2009; **16:** 878–886.
4. Wouters MW, Karim-Kos HE, le Cessie S, *et al.* Centralization of esophageal cancer surgery: does it improve clinical outcome? *Ann Surg Oncol* 2009; **16:** 1789–1798.
5. DeBerardinis RJ, Lum JJ, Hatzivassiliou G, *et al.* The biology of cancer: metabolic reprogramming fuels cell growth and proliferation. *Cell Metab* 2008; **7:** 11–20.
6. Plathow C, Weber WA. Tumor cell metabolism imaging. *J Nucl Med* 2008; **49**(suppl 2): 43S–63S.
7. Sohda M, Kato H, Suzuki S, *et al.* ^{18}F-FAMT-PET is useful for the diagnosis of lymph node metastasis in operable esophageal squamous cell carcinoma. *Ann Surg Oncol* 2010; **17:** 3181–3186.
8. Yasuda T, Higuchi I, Yano M, *et al.* The impact of ^{18}F-fluorodeoxyglucose positron emission tomography positive lymph nodes on postoperative recurrence and survival in resectable thoracic esophageal squamous cell carcinoma. *Ann Surg Oncol* 2012; **19:** 652–660.
9. Kroemer G, Pouyssegur J. Tumor cell metabolism: cancer's Achilles' heel. *Cancer Cell* 2008; **13:** 472–482.
10. Mitsuishi Y, Taguchi K, Kawatani Y, *et al.* Nrf2 redirects glucose and glutamine into anabolic pathways in metabolic reprogramming. *Cancer Cell* 2012; **22:** 66–79.
11. Sawayama H, Ishimoto T, Sugihara H, *et al.* Clinical impact of the Warburg effect in gastrointestinal cancer (review). *Int J Oncol* 2014; **45:** 1345–1354.
12. Mitsuishi Y, Motohashi H, Yamamoto M. The Keap1–Nrf2 system in cancers: stress response and anabolic metabolism. *Front Oncol* 2012; **2:** 200.
13. Lee AC, Fenster BE, Ito H, *et al.* Ras proteins induce senescence by altering the intracellular levels of reactive oxygen species. *J Biol Chem* 1999; **274:** 7936–7940.
14. Vafa O, Wade M, Kern S, *et al.* c-Myc can induce DNA damage, increase reactive oxygen species, and mitigate p53 function: a mechanism for oncogene-induced genetic instability. *Mol Cell* 2002; **9:** 1031–1044.

15. Nogueira V, Park Y, Chen CC, *et al.* Akt determines replicative senescence and oxidative or oncogenic premature senescence and sensitizes cells to oxidative apoptosis. *Cancer Cell* 2008; **14:** 458–470.
16. Cairns RA, Harris IS, Mak TW. Regulation of cancer cell metabolism. *Nat Rev Cancer* 2011; **11:** 85–95.
17. Sabharwal SS, Schumacker PT. Mitochondrial ROS in cancer: initiators, amplifiers or an Achilles' heel? *Nat Rev Cancer* 2014; **14:** 709–721.
18. Itoh K, Chiba T, Takahashi S, *et al.* An Nrf2/small Maf heterodimer mediates the induction of phase II detoxifying enzyme genes through antioxidant response elements. *Biochem Biophys Res Commun* 1997; **236:** 313–322.
19. Uruno A, Motohashi H. The Keap1–Nrf2 system as an *in vivo* sensor for electrophiles. *Nitric Oxide* 2011; **25:** 153–160.
20. Singh A, Misra V, Thimmulappa RK, *et al.* Dysfunctional KEAP1–NRF2 interaction in non-small-cell lung cancer. *PLoS Med* 2006; **3:** e420.
21. Shibata T, Ohta T, Tong KI, *et al.* Cancer related mutations in NRF2 impair its recognition by Keap1–Cul3 E3 ligase and promote malignancy. *Proc Natl Acad Sci U S A* 2008; **105:** 13568–13573.
22. Wang R, An J, Ji F, *et al.* Hypermethylation of the *Keap1* gene in human lung cancer cell lines and lung cancer tissues. *Biochem Biophys Res Commun* 2008; **373:** 151–154.
23. Solis LM, Behrens C, Dong W, *et al.* Nrf2 and Keap1 abnormalities in non-small cell lung carcinoma and association with clinicopathologic features. *Clin Cancer Res* 2010; **16:** 3743–3753.
24. Singh A, Boldin-Adamsky S, Thimmulappa RK, *et al.* RNAi-mediated silencing of nuclear factor erythroid-2-related factor 2 gene expression in non-small cell lung cancer inhibits tumor growth and increases efficacy of chemotherapy. *Cancer Res* 2008; **68:** 7975–7984.
25. Zhang P, Singh A, Yegnasubramanian S, *et al.* Loss of Kelch-like ECH-associated protein 1 function in prostate cancer cells causes chemoresistance and radioresistance and promotes tumor growth. *Mol Cancer Ther* 2010; **9:** 336–346.
26. Ludtmann MH, Angelova PR, Zhang Y, *et al.* Nrf2 affects the efficiency of mitochondrial fatty acid oxidation. *Biochem J* 2014; **457:** 415–424.
27. DeNicola GM, Chen PH, Mullarky E, *et al.* NRF2 regulates serine biosynthesis in non-small cell lung cancer. *Nat Genet* 2015; **47:** 1475–1481.
28. Xu IM, Lai RK, Lin SH, *et al.* Transketolase counteracts oxidative stress to drive cancer development. *Proc Natl Acad Sci U S A* 2016; **113:** E725–E734.
29. Cancer Genome Atlas Research Network; Analysis Working Group: Asan University; BC Cancer Agency, *et al.* Integrated genomic characterization of oesophageal carcinoma. *Nature* 2017; **541:** 169–175.
30. Rice TW, Blackstone EH, Rusch VW. 7th Edition of the AJCC *Cancer Staging Manual*: esophagus and esophagogastric junction. *Ann Surg Oncol* 2010; **17:** 1721–1724.
31. Hiyoshi Y, Kamohara H, Karashima R, *et al.* MicroRNA-21 regulates the proliferation and invasion in esophageal squamous cell carcinoma. *Clin Cancer Res* 2009; **15:** 1915–1922.
32. Hayes JD, Dinkova-Kostova AT. The Nrf2 regulatory network provides an interface between redox and intermediary metabolism. *Trends Biochem Sci* 2014; **39:** 199–218.
33. Genov M, Kreiseder B, Nagl M, *et al.* Tetrahydroanthraquinone derivative (±)-4-deoxyaustrocortilutein induces cell cycle arrest and apoptosis in melanoma cells via upregulation of p21 and p53 and downregulation of NF-kappaB. *J Cancer* 2016; **7:** 555–568.
34. Aquilano K, Baldelli S, Ciriolo MR. Glutathione: new roles in redox signaling for an old antioxidant. *Front Pharmacol* 2014; **5:** 196.
35. Karnoub AE, Weinberg RA. Ras oncogenes: split personalities. *Nat Rev Mol Cell Biol* 2008; **9:** 517–531.
36. Coulthard LR, White DE, Jones DL, *et al.* p38(MAPK): stress responses from molecular mechanisms to therapeutics. *Trends Mol Med* 2009; **15:** 369–379.
37. Lee J, Sun C, Zhou Y, *et al.* p38 MAPK-mediated regulation of Xbp1s is crucial for glucose homeostasis. *Nat Med* 2011; **17:** 1251–1260.
38. Hanahan D, Weinberg RA. Hallmarks of cancer: the next generation. *Cell* 2011; **144:** 646–674.
39. Warburg O, Wind F, Negelein E. The metabolism of tumors in the body. *J Gen Physiol* 1927; **8:** 519–530.
40. Kim YR, Oh JE, Kim MS, *et al.* Oncogenic *NRF2* mutations in squamous cell carcinomas of oesophagus and skin. *J Pathol* 2010; **220:** 446–451.
41. Shibata T, Kokubu A, Saito S, *et al. NRF2* mutation confers malignant potential and resistance to chemoradiation therapy in advanced esophageal squamous cancer. *Neoplasia* 2011; **13:** 864–873.
42. Yamamoto S, Inoue J, Kawano T, *et al.* The impact of miRNA-based molecular diagnostics and treatment of NRF2-stabilized tumors. *Mol Cancer Res* 2014; **12:** 58–68.
43. Altman BJ, Stine ZE, Dang CV. From Krebs to clinic: glutamine metabolism to cancer therapy. *Nat Rev Cancer* 2016; **16:** 619–634.
44. Ishimoto T, Nagano O, Yae T, *et al.* CD44 variant regulates redox status in cancer cells by stabilizing the xCT subunit of system xc^- and thereby promotes tumor growth. *Cancer Cell* 2011; **19:** 387–400.
45. Blair SL, Heerdt P, Sachar S, *et al.* Glutathione metabolism in patients with non-small cell lung cancers. *Cancer Res* 1997; **57:** 152–155.
46. Wang W, Kryczek I, Dostal L, *et al.* Effector T cells abrogate stroma-mediated chemoresistance in ovarian cancer. *Cell* 2016; **165:** 1092–1105.
47. Lu SC. Regulation of glutathione synthesis. *Mol Aspects Med* 2009; **30:** 42–59.

SUPPLEMENTARY MATERIAL ONLINE

Supplementary figure legends

Figure S1. Immunohistochemistry for Nrf2 expression in oesophageal cancer tissues and the relationship between Nrf2 expression status in oesophageal cancer and overall survival

Figure S2. Mutation status of *Nrf2* and *Keap1* in oesophageal cancer cell lines from the COSMIC database and CCLE project; modulation of *Nrf2* mRNA and protein levels in TE-11 cells

Figure S3. Cell cycle analyses performed by flow cytometry

Figure S4. Fold change of the intensity of cleaved caspase-3, phospho-p38 MAPK, and cyclin D1 assessed by western blotting

Figure S5. Assessment of ROS in TE-11 cells using CellROX Green Reagent and immunohistochemistry for Nrf2, cyclin D1, and Ki-67 in resected oesophageal cancer specimens

Figure S6. Amino acid content in TE-11 cells treated with siCtrl and siNrf2; GSH levels in TE-1, -9, and -11 cells; and concentrations of metabolites in the pentose phosphate pathway

Table S1. Primers used for qPCR

Table S2. Expression of Nrf2 in oesophageal cancer specimens and association with clinical and tumour features

Table S3. GSEA analysis of KEGG glutathione metabolism from GEO profiles